



Contents lists available at ScienceDirect

## Journal of Steroid Biochemistry and Molecular Biology

journal homepage: [www.elsevier.com/locate/jsmb](http://www.elsevier.com/locate/jsmb)

# Chemical synthesis and biochemical properties of cholestane-5 $\alpha$ ,6 $\beta$ -diol-3-sulfonate: A non-hydrolysable analogue of cholestane-5 $\alpha$ ,6 $\beta$ -diol-3-sulfate

Philippe de Médina<sup>a,b,c,\*</sup>, Silia Ayadi<sup>a,b,1</sup>, Régis Soules<sup>a,b,c</sup>, Bruno Payre<sup>d</sup>, Sandrine Rup-Jacques<sup>e</sup>, Sandrine Silvente-Poirot<sup>a,b,c,\*</sup>, Mohammad Samadi<sup>e,\*\*</sup>, Marc Poirot<sup>a,b,c,\*</sup>

<sup>a</sup> Cancer Research Center of Toulouse (CRCT), Inserm, CNRS, University of Toulouse, Team INOV: Cholesterol Metabolism and Therapeutic Innovations, Toulouse, France

<sup>b</sup> Equipe labellisée par la Ligue Nationale contre le Cancer, France

<sup>c</sup> French network for Nutrition physical Activity And Cancer Research (NACRe network), France

<sup>d</sup> Centre de Microscopie Electronique Appliquée à la Biologie, Faculté de Médecine Rangueil, Toulouse, France

<sup>e</sup> Laboratory of Chemistry and Physics Multi-Scale Approach to Complex Environments, Department of Chemistry, University Lorraine, 57070 Metz, France

## ARTICLE INFO

## Key words:

Sterols  
Oxysterol  
Oxysterol sulfate  
Cholesterol  
Uptake  
Metabolism  
Cell death MLB  
Cancer  
NPC1  
Proliferation  
Cell death  
Autophagy

## ABSTRACT

Cholestane-3 $\beta$ ,5 $\alpha$ ,6 $\beta$ -triol (CT) is a primary metabolite of 5,6-epoxycholesterols (5,6-EC) that is catalyzed by the cholesterol-5,6-epoxide hydrolase (ChEH). CT is a well-known biomarker for Niemann-Pick disease type C (NPC), a progressive inherited neurodegenerative disease. On the other hand, CT is known to be metabolized by the 11 $\beta$ -hydroxysteroid-dehydrogenase of type 2 (11 $\beta$ -HSD2) into a tumor promoter named oncosterone that stimulates the growth of breast cancer tumors. Sulfation is a major metabolic transformation leading to the production of sulfated oxysterols. The production of cholestane-5 $\alpha$ ,6 $\beta$ -diol-3 $\beta$ -O-sulfate (CDS) has been reported in breast cancer cells. However, no data related to CDS biological properties have been reported so far. These studies have been hampered because sulfate esters of sterols and steroids are rapidly hydrolyzed by steroid sulfatase to give free steroids and sterols. In order to get insight into the biological properties of CDS, we report herein the synthesis and the characterization of cholestane-5 $\alpha$ ,6 $\beta$ -diol-3 $\beta$ -sulfonate (CDSN), a non-hydrolysable analogue of CDS. We show that CDSN is a potent inhibitor of 11 $\beta$ -HSD2 that blocks oncosterone production on cell lysate. The inhibition of oncosterone biosynthesis of a whole cell assay was observed but results from the blockage by CDSN of the uptake of CT in MCF-7 cells. While CDSN inhibits MCF-7 cell proliferation, we found that it potentiates the cytotoxic activity of post-lanosterol cholesterol biosynthesis inhibitors such as tamoxifen and PBPE. This effect was associated with an increase of free sterols accumulation and the appearance of giant multilamellar bodies, a structural feature reminiscent of Type C Niemann-Pick disease cells and consistent with a possible inhibition by CDSN of NPC1. Altogether, our data showed that CDSN is biologically active and that it is a valuable tool to study the biological properties of CDS and more specifically its impact on immunity and viral infection.

**Abbreviations:** 5,6 $\alpha$ , EC, 5,6 $\alpha$ , epoxycholesterols; 5,6 $\beta$ -EC, 5,6 $\beta$ -epoxycholesterols; 11 $\beta$ -HSD2, 11 $\beta$ -hydroxysteroid-dehydrogenase of type 2; CDS, cholestane-5 $\alpha$ ,6 $\beta$ -diol-3 $\beta$ -O-sulfate; CDSN, cholestane-5 $\alpha$ ,6 $\beta$ -diol-3 $\beta$ -sulfonate; ChEH, cholesterol-5,6-epoxide hydrolase; CT, cholestane-3 $\beta$ ,5 $\alpha$ ,6 $\beta$ -triol; Ez, Ezetimibe; NPC, Niemann-Pick type C; OCDO, oncosterone, 6-oxo-cholestan-3 $\beta$ ,5 $\alpha$ -diol.

\* Corresponding authors at: Cancer Research Center of Toulouse (CRCT), Inserm, CNRS, University of Toulouse, Team INOV: Cholesterol Metabolism and Therapeutic Innovations, Toulouse, France

\*\* Correspondence to: Laboratory of Chemistry and Physics Multi-Scale Approach to Complex Environments, Department of Chemistry, University Lorraine, Metz, France.

E-mail addresses: [philippe.de-medina@inserm.fr](mailto:philippe.de-medina@inserm.fr) (P. de Médina), [sandrine.poirot@inserm.fr](mailto:sandrine.poirot@inserm.fr) (S. Silvente-Poirot), [mohammad.samadi@univ-lorraine.fr](mailto:mohammad.samadi@univ-lorraine.fr) (M. Samadi), [marc.poirot@inserm.fr](mailto:marc.poirot@inserm.fr) (M. Poirot).

<sup>1</sup> these authors contribute equally to this work

<https://doi.org/10.1016/j.jsmb.2023.106396>

Received 30 June 2023; Received in revised form 22 August 2023; Accepted 4 September 2023

Available online 6 September 2023

0960-0760/© 2023 Elsevier Ltd. All rights reserved.

## 1. Introduction

Oxysterols (OS) represent an expanding family of bioactive oxygenated cholesterol metabolites that impact on a plethora of diseases including atherosclerosis, cancer, neurodegenerative diseases and aging [1,2]. Depending on their chemical structures, these metabolites can exert their biological properties through various molecular mechanisms that could involve either nuclear receptors (e.g., LXR, ROR, ER $\alpha$ , GR) [3–6], G-protein coupled receptors (e.g., SMO, CXCR2, EBI2) [7–11], enzymes (e.g., SOAT/ACAT, ChEH and HMGCoA reductase) [12–15] or transporters (e.g., ions transporters, INSIG, oxysterol binding proteins, NPC1 and NPC1L1) [16–21]. Cholestane-3 $\beta$ ,5 $\alpha$ ,6 $\beta$ -triol (CT) and its obligatory precursors 5,6-epoxycholesterols (5,6-ECs) [22] occupy an important place among the oxysterol family, because 5,6-EC are among the major OS found in processed food and in circulating blood [4,15,23]. In addition CT is a biomarker of several pathologies such as Niemann-Pick type C (i.e., an inherited neurodegenerative disease), allergic asthma and potentially breast cancers [24–26], and a potential marker of other diseases [27–31]. Looking at the biological properties of CT, both beneficial and deleterious effects have been reported. For example, CT displays antiproliferative, cytotoxic and mutagenic activities and promote vascular smooth muscle cells calcification, a process associated with atherosclerosis [32,33]. On the other hand, this OS acts as a neuroprotectant and an anti-epileptic agent [34,35]. Although CT can be formed through the acidic hydrolysis of 5,6-epoxycholestan-3 $\beta$ -ol (5,6-ECs) in strong acidic conditions, in mammalian tissues their hydrolysis requires the obligatory intervention of a microsomal enzyme: the cholesterol-5,6-epoxide hydrolase (ChEH) [14], indeed, the epoxide ring of 5,6-EC was surprisingly found extremely stable towards the attack of nucleophilic compounds by contrast with other aliphatic epoxides [23,36]. Interestingly, in cancer, CT was shown to be oxidized by the 11 $\beta$ -hydroxysteroid-dehydrogenase of type 2 (11 $\beta$ -HSD2) to form an oncometabolite named oncosterone, that promotes breast cancer (BC) proliferation and invasiveness both in vitro and in vivo [3,22,37]. CT was also shown to be sulfated in cells by the sulfotransferase SULT2B1b leading to the production of cholestane-5 $\alpha$ ,6 $\beta$ -diol-3 $\beta$ -sulfate (CDS) [38–40]. While genetic evidences supported an inactivation of steroids and sterols through sulfation [41,42], other data evidenced that sulfation generates biologically active signaling molecules. Cholesterol sulfate was shown to be important in keratinocyte physiology [43] and to control tumor infiltration of T cells [44]. The sulfation of side chain OS led to compounds that display trophic and proliferative properties [45]. B-ring oxysterols led to the production of LXR antagonists on a gene reporter assay [46]. Interestingly the sulfated form of 5,6 $\alpha$ -EC was shown to control BC cell differentiation and death [39,47]. The 25-hydroxycholesterol-3-sulfate, a sulfated side chain oxysterol, was shown to be an epigenetic regulator that activates fatty acid oxidation, and this compound is under clinical evaluation for the treatment of Non-Alcoholic Steatohepatitis and Alcoholic Hepatitis [48–50]. In addition, the expression of SULT2B1b in tumors inhibits tumor growth and restore antitumor immune response highlighting the implication of a SULT2B1/LXR pathway potentially involving yet unidentified sulfated

OS [51]. We previously reported that the sulfated metabolite of CT (cholestane-5 $\alpha$ ,6 $\beta$ -diol-3 $\beta$ -sulfate; CDS; Fig. 1A) is produced in breast cancer cells highlighting that this compound is a metabolite and a modulator of LXR signaling [39]. Despite this observation, studies aiming to evaluate the biological properties of CDS have never been reported to date. Studies on CDS have been hampered because sulfated (oxy)sterols are rapidly hydrolyzed by the steroid sulfatase (STS) which is widely expressed in various tissues and cancer cells (Fig. 1A) [39,52]. To circumvent this problem, we decided to synthesize a non-hydrolysable analogue of CDS. The strategy to produce a non-hydrolysable CDS analogue is by removing the oxygen in 3 $\beta$  position of steroid backbone involved in the esterification to eliminate the point of cleavage by STS (Fig. 1) as previously reported for estrone sulfate [53], and we report herein for the first time the chemical synthesis of cholestane-5 $\alpha$ ,6 $\beta$ -diol-3 $\beta$ -sulfonate (CDSN) (Fig. 1B) as a stable and non-hydrolysable chemical analogue of CDS. We evaluate the impact of CDSN on BC cells on the biosynthesis of oncosterone, on the cellular uptake of several OS and on cell fate.

## 2. Experimental section

### 2.1. General

All reagents were obtained from commercial suppliers and used without further purification. PBPE (1-[2-(4-benzylphenoxy)ethyl]pyrrolidine) was produced as reported before [54]. Flash chromatography was carried out using silica gel (Merck Kieselgel 60, 230–400 mesh). Thin layer chromatography (TLC) analyses were performed on thin-layer analytical plates 60 F<sub>254</sub> (Merck). Melting points were measured on a Stuart melting point apparatus SMP30. Infrared (IR) spectra were recorded on a Nicolet iS5 FT-IR spectrometer. <sup>1</sup>H and <sup>13</sup>C NMR spectra were recorded with a Bruker AvanceNeo 400 spectrometer and are shown on the Supplementary material section.

### 2.2. Chemical synthesis of cholestane-5 $\alpha$ ,6 $\beta$ -diol-3 $\beta$ -sulfonate (CDSN)

**Thiocholesterol (4):** Thiocholesterol was prepared according to the procedure described by King and al [36], from cholesterylisothiuronium *p*-toluenesulfonate [55] **2** (2.156 g, 3.5 mmol). The solid crude product was purified over silica gel using hexane as eluent to yield **4** as a white solid (1.210 g; 86 %). mp 95.5 °C (lit [36] 97.5 °C). IR (neat)  $\nu$ : 2930, 2899, 2865, 2849, 1465, 1375 cm<sup>-1</sup>. <sup>1</sup>H NMR (400 MHz, CDCl<sub>3</sub>)  $\delta$  5.31 (m, 1 H, H-6), 2.69 (m, 1 H, H-3), 2.31 (m, 2 H, H-5), 1.00 (s, 3 H, 19-CH<sub>3</sub>), 0.91 (d, *J* = 6.6 Hz, 3 H, 21-CH<sub>3</sub>), 0.86 (dd, *J* = 6.6, 1.8 Hz, 6 H, 26-CH<sub>3</sub> and 27-CH<sub>3</sub>), 0.67 (s, 3 H, 18-CH<sub>3</sub>). <sup>13</sup>C NMR (101 MHz, CDCl<sub>3</sub>)  $\delta$  142.06, 121.19, 56.90, 56.30, 50.35, 44.36, 42.45, 40.08, 39.90, 39.67, 39.60, 36.49, 36.34, 35.94, 34.23, 31.95 (CH<sub>2</sub>), 31.95 (CH), 28.38, 28.17, 24.42, 23.98, 22.97, 22.71, 21.05, 19.48, 18.87, 12.00. the <sup>1</sup>H and <sup>13</sup>C NMR data were identical to that reported in lit [38] MS (EI, CH<sub>2</sub>Cl<sub>2</sub>): *m/z*: 402 ([M]<sup>+</sup>, 43 %).

**5 $\alpha$ ,6 $\beta$ -dihydroxy-cholesteryl sulfonate (5):**

**Method A:** A solution of 35 % H<sub>2</sub>O<sub>2</sub> (1 ml) was dissolved in 98%

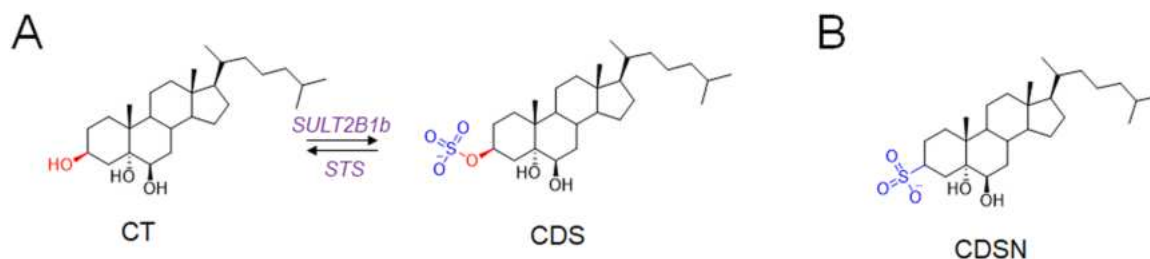


**Fig. 1.** A) The reaction of sulfation of cholestane-3 $\beta$ ,5 $\alpha$ ,6 $\beta$ -triol (CT) is catalyzed by the sulfotransferase SULT2B1b to give cholestane-5 $\alpha$ ,6 $\beta$ -diol-3 $\beta$ -sulfate (CDS). The desulfation of CDS is catalyzed by the steroid sulfatase (STS). B) Chemical structure of cholestane-5 $\alpha$ ,6 $\beta$ -diol-3 $\beta$ -sulfonate (CDSN), a non-hydrolysable analogue of CDS.

formic acid (4 ml) at 0 °C and the mixture was stirred at rt for 1 h to afford peroxyformic acid. To this was added a solution of thiocholesterol 4 (1 mmol, 402 mg) in CH<sub>2</sub>Cl<sub>2</sub> (5 ml) at 0 °C. The reaction was stirred at rt overnight. The reaction content was transferred to a 250 ml flask and the solvent was carefully (foam formation) evaporated below 25 °C and dried under vacuum. The residue was dissolved with 20 ml of MeOH and heated at 60 °C in a water-bath for 1 h. The solvent was evaporated and purified on silica gel using CH<sub>2</sub>Cl<sub>2</sub>-MeOH (80–20 then 70–30) to yield 5 as a white solid (446 mg; 92%),

**Method B:** A solution of 35 % H<sub>2</sub>O<sub>2</sub> (1 ml) was dissolved in 98% formic acid (1 ml) at 0 °C and the mixture was stirred at rt for 1 h to afford peroxyformic acid. To this was added a solution of thiocholesterol 4 (1 mmol, 402 mg) in THF (8 ml) at 0 °C and stirred at rt for 1 h. The solution was warmed to 50–60 °C in a water-bath for 3 h and stirred at rt overnight. The solvent was evaporated and treated as described above to yield 5 as a white solid (460 mg; 95%), mp 275.3 °C. IR (neat)  $\nu$ : 3404, 2932, 2866, 1228, 1164, 1048 cm<sup>-1</sup>. <sup>1</sup>H NMR (400 MHz, MeOD)  $\delta$  3.49 (d,  $J$  = 3.4 Hz, 1 H, H-6), 3.20 (tt,  $J$  = 12.5, 4.5 Hz, 1 H, H-3), 2.37 (t,  $J$  = 13.1 Hz, 1 H, 2-Hax), 1.15 (s, 3 H, 19-CH<sub>3</sub>), 0.94 (d,  $J$  = 6.4 Hz, 3 H, 21-CH<sub>3</sub>), 0.88 (d,  $J$  = 6.5 Hz, 6 H, 26-CH<sub>3</sub> and 27-CH<sub>3</sub>), 0.71 (s, 3 H, 18-CH<sub>3</sub>). <sup>13</sup>C NMR (101 MHz, MeOD)  $\delta$  76.42, 75.37, 57.67, 57.51, 56.14, 46.66, 43.89, 41.49, 40.70, 39.35, 37.38, 37.15, 35.45, 34.10, 33.62, 31.63, 29.34, 29.14, 25.19, 24.94, 23.41, 23.20, 22.95, 22.08, 19.24, 17.00, 12.61.

### 2.3. Cell culture

MCF7 cells were chosen because they express a functional SULT2B1b enzyme [39]. HEK293T cells were chosen for transfection assays and overexpression of HSD11B2 as reported in [56]. MCF-7 and HEK293T cells were from the American Tissue Culture Collection and cultured until passage 30. MCF-7 cells were grown in RPMI 1640 supplemented with 5 % fetal bovine serum (FBS). HEK293T cells were grown in DMEM 10 % FBS. All media were supplemented with penicillin and streptomycin (50 U/ml). Cells were cultured in a humidified atmosphere with 5 % CO<sub>2</sub> at 37 °C. Cell lines were tested once a month for mycoplasma contamination using Mycoalert Detection (Lonza).

### 2.4. Measure of sterol metabolism in MCF-7 Cells

We have used MCF-7 cells for whole cell oncosterone biosynthesis assays from [<sup>14</sup>C]-CT as described before [37]. MCF-7 cells were plated into six-well plates (1.5 × 10<sup>5</sup> cells per well) in the appropriate complete medium. Two days after seeding, this medium was replaced with complete medium and cells were treated with 1 μM [<sup>14</sup>C]-CT (26 mCi/mmol; 0.052 μCi/well) for 5 h in the presence or absence of CDSN at 20 μM. After incubation, cells were washed and scraped, and neutral lipids were extracted with a chloroform-methanol mixture as described previously and then separated by TLC using either ethyl acetate as the eluent [57]. The radio-labeled sterols were revealed by autoradiography. For quantification, silica zones at the expected R<sub>f</sub> values corresponding to authentic [<sup>14</sup>C]-labeled standards were scraped and radioactivity was measured using a β-counter.

### 2.5. Cell transfection

HEK-293 T cells (5.10<sup>6</sup>) were transfected with 5 μg of the plasmid pCMV6-XL5 HSD2 (SC122552, OriGene Technologies, Inc., Rockville, MD, USA) using the Neon Transfection System (Thermo Fisher Scientific, Waltham, MA, USA) with 2 pulses at 1300 V for 20 ms. 48 h after transfection, the media was replaced by DMEM without phenol red supplemented with 10 % dextran-coated charcoal-stripped FBS. Cells were harvested 72 h after transfection, washed with PBS and stored at – 80 °C.

### 2.6. Measure of oncosterone biosynthesis inhibition by CDSN

We have chosen to test the cell lysate from HEK293T cells transfected with a plasmide encoding 11β-HSD2 to measure the impact of inhibitors of oncosterone biosynthesis from [<sup>14</sup>C]-CT at the enzyme level [37]. Cell lysates were prepared from HEK293T cells transiently expressing human 11β-HSD2 as described before [37]. Briefly, 2.10<sup>6</sup> cells were resuspended in 150 μL of activity buffer (Tris-HCl 25 mM PH 7.4, glycerol 20%, sucrose 25 mM, NaCl 200 mM, MgCl<sub>2</sub> 1 mM, CaCl<sub>2</sub> 1 mM) with 1% protease inhibitor mixture (Sigma-Aldrich). Cells were lysed by four cycles of freeze/thaw (nitrogen-rt) and samples were centrifuged at 10,000 rpm for 10 min at 4 °C. The supernatant was collected, aliquoted and stored at – 80 °C before use. Protein concentration was measured using the Bradford method. The enzymatic activity was measured in an 11β-HSD2 activity buffer (final volume 0.2 ml) containing the substrate ([<sup>14</sup>C]-CT (1 μM), cell lysate proteins (20 μg), NAD<sup>+</sup> (0.5 mM) and DMSO 1 % in the absence or presence of the tested compounds. After 10 min of incubation at 37 °C, the reaction was stopped by immersing the sample in ice-water and adding 1.5 ml chloroform/methanol (2:1) and 300 μL of aqueous KCl (8.8 %). The organic layer was washed with water (1 ml) and reduced to dryness under a flux of nitrogen. Lipids were then separated by TLC using either ethyl acetate as the eluent. The radioactive sterols were revealed by autoradiography. For quantification, silica zones at the expected R<sub>f</sub> values corresponding to authentic [<sup>14</sup>C]-labeled standards were scraped and radioactivity was measured using a β-counter (tri-carb; Perkin-Elmer).

### 2.7. Uptake of cholesterol, 5,6-ECs, and CT

MCF-7 cells were plated into twelve-well plates (7.5 × 10<sup>4</sup> cells per well) in the appropriate complete medium. Four days after seeding, the medium was replaced with 5 % FBS medium or medium without FBS and cells were incubated with [<sup>14</sup>C]-cholesterol, [<sup>14</sup>C]-5,6α-EC, [<sup>14</sup>C]-5,6β-EC or [<sup>14</sup>C]-CT (1 μM; 26 mCi/mmol; 0.026 μCi/well) in the presence or absence of 40 μM Ezetimibe (Ez) (Sigma-Aldrich) or 20 μM of CDSN, for 5 h. Then, cells were washed with PBS and were resuspended in 1 ml of SDS 0.1 %. Radioactivity was measured using a β-counter (tri-carb; Perkin-Elmer).

### 2.8. Cell death assay

MCF-7 cells were seeded in RPMI with 5 % FBS into 6-well plates at 1.5 × 10<sup>5</sup> cells per well. The cells were then treated with solvent vehicle (0.1 % ethanol/0.1 % DMSO), 2.5 μM Tam or 10 μM PBPE alone or in the presence of 10 μM CDSN. Cell death was determined by the Trypan blue exclusion assay. The cells were trypsinized and resuspended in the Trypan blue solution (0.25 % (w/v) in PBS) and counted in a Malassez cell under a light microscope.

### 2.9. Filipin staining procedures

Cells were grown on glass coverslips and treated with drugs for 72 h and then fixed with 3.7 % paraformaldehyde for 15 min at room temperature followed by washing twice with PBS (Euromedex), and stained with filipin (50 mg/ml) for 75 min at room temperature followed by washing twice with PBS as described before [58]. Cells were analysed using a Nikon eclipse 90i microscope. The pixel intensities of the images were measured using NIH Image software and reported on a graph as in [59].

### 2.10. Transmission electron microscopy

Cells were fixed with 2 % glutaraldehyde in 0.1 mol/L Sorensen phosphate buffer (pH 7.4) for 1 h and washed with the Sorensen phosphate buffer (0.1 mol/L) for 12 h. The cells were then postfixed with 1 % OsO<sub>4</sub> in Sorensen phosphate buffer (0.05 mol/L Sorensen phosphate

buffer, 0.25 mol/L glucose, 1 %  $\text{OsO}_4$ ) for 1 h. The cells were then washed twice with distilled water and prestained with an aqueous solution of 2 % uranyl acetate for 12 h. Samples were then treated exactly as described previously [60].

### 2.11. Statistical analysis

Values are the mean  $\pm$  S.E. of three independent experiments each carried out in duplicate. Statistical analysis was carried out using a Student's *t*-test for unpaired variables. \*, \*\* and \*\*\* in the figures refer to statistical probabilities (*P*) of < 0.05, < 0.01 and < 0.001, respectively, compared with control cells that received solvent vehicle alone.

## 3. Results and discussion

### 3.1. Chemical synthesis of CDSN

The chemical synthesis of CDSN is shown in Fig. 2. Initially, we examined the preparation of cholesteryl sulfonate **3** by oxidation of cholesterylisothiuronium *p*-toluenesulfonate **2** [55] with performic acid according to Yoder procedure [41].  $^1\text{H}$  NMR analysis of **3** reveals the presence of *p*-toluenesulfonic acid as by product. Tentative to remove *p*-toluenesulfonic acid which accompanied compound **3**, either by crystallization or purification over silica gel was unsuccessful. To circumvent this problem, we turned to the oxidation of thiocholesterol **4**, which was prepared from **2** by alkali hydrolysis [61]. Thus, the oxidation of thiocholesterol with performic acid in  $\text{CH}_2\text{Cl}_2$  or THF produced a mixture of **3** and the deprotected sulfonate **5**. Heating the resulting mixture at 60 °C in MeOH affect the deformylation of **3**, which is catalyzed by the sulfonic acid [62] moiety and furnished the desired 5 $\alpha$ ,6 $\beta$ -dihydroxy-cholesteryl sulfonate **5** (Fig. 2). In conclusion, the synthesis of 5 $\alpha$ ,6 $\beta$ -dihydroxy-cholesteryl sulfonate **5** was achieved in four steps from commercially available cholesterol **1**. The facile deprotection of **3** is due to the presence of a sulfonic acid moiety, avoiding the use of a strong base (e.g. NaOH, KOH,  $\text{K}_2\text{CO}_3$ ) is worthy-mentioning.  $^1\text{H}$  NMR and  $^{13}\text{C}$  NMR spectra are presented in [supplementary material](#).

### 3.2. CDSN is an inhibitor of oncoesterone biosynthesis

We have previously demonstrated that CT is metabolized toward the oncometabolite oncoesterone through 11 $\beta$ -HSD2 [37]. The inhibition of oncoesterone production constitutes a putative new therapeutic strategy for the treatment of BC [3,22]. Consequently, we evaluated if CDSN can inhibit oncoesterone production. We evaluated the impact of CDSN on oncoesterone production catalyzed by 11 $\beta$ -HSD2. The measure of the

oncoesterone synthase activity was carried out on cell lysate from HEK-293 T transiently transfected with a plasmid encoding the human 11 $\beta$ -HSD2 (HEK293T-11HSD2 lysate). The conversion of [ $^{14}\text{C}$ ]-CT into [ $^{14}\text{C}$ ]-Oncoesterone in HEK293-11HSD2 lysate was measured alone or with increasing concentrations of CDSN ranging from 1 to 10  $\mu\text{M}$ . CDSN inhibits the production of [ $^{14}\text{C}$ ]-Oncoesterone from [ $^{14}\text{C}$ ]-CT in a dose-dependent manner ( $\text{IC}_{50} = 2.55 \pm 0.63 \mu\text{M}$ ) (Fig. 3A-B). Consequently, CDSN is a potent inhibitor of oncoesterone synthase activity.

### 3.3. Impact of CDSN on CT metabolism in MCF-7 cells

We previously reported that the human BC cell line MCF-7 cells expressed the SULT2B1b protein, produced sulfated OS [30] and responded to the stimulation of sulfated OS. We have thus chosen this cell line to study the effect of CDSN. We measured the impact of CDSN on oncoesterone (OCDO) formation on a whole cell assay by incubating MCF-7 cells with [ $^{14}\text{C}$ ]-CT alone or in the presence of 20  $\mu\text{M}$  CDSN for 5 h. After 48 hr, and in the absence of CDSN,  $19 \pm 6$  % of the radioactivity was incorporated into cells (Fig. 4A). The intracellular radioactivity corresponds at  $16 \pm 2$  % to [ $^{14}\text{C}$ ]-OCDO formed by 11 $\beta$ -HSD2 in MCF-7 cells (Fig. 4B). Surprisingly, the treatment of cells with CDSN triggers a strong diminution of the intracellular radioactivity (Fig. 4A) whereas the percentage of intracellular [ $^{14}\text{C}$ ]-OCDO was not affected by CDSN (Fig. 4B). Indeed, CDSN reduces the intracellular level of both [ $^{14}\text{C}$ ]-CT and [ $^{14}\text{C}$ ]-OCDO by 69 % and 44 % respectively in MCF-7 cells (Fig. 4C). These results showed that CDSN does not inhibit the biosynthesis of oncoesterone on a whole cell assay but inhibits CT uptake in MCF-7 cells.

### 3.4. Impact of CDSN on oxysterols and cholesterol uptake in breast cancer cells

To get more insight on the ability of CDSN to inhibit the cellular uptake of OS, we evaluate the impact of CDSN compared with ezetimibe (Ez) (i.e., a well-known inhibitor of NPC1L1) that was shown to inhibit the uptake of B-ring OS [63]. MCF-7 cells were treated with [ $^{14}\text{C}$ ]-cholesterol, [ $^{14}\text{C}$ ]-5,6 $\alpha$ -EC, [ $^{14}\text{C}$ ]-5,6 $\beta$ -EC and [ $^{14}\text{C}$ ]-CT alone or in the presence of 20  $\mu\text{M}$  CDSN or with 40  $\mu\text{M}$  Ez for 5 h. Cells were then lysed by SDS 0.1 % and the intracellular radioactivity was measured. We found that Ez slightly reduces the uptake of cholesterol by approximately 20 % but did not inhibit the uptake of 5,6 $\alpha$ -E, 5,6 $\beta$ -EC and CT. By contrast, we found that CDSN induced of 70 % reduction of cholesterol uptake and a 17 %, 24 % and 36 % inhibition of 5,6 $\alpha$ -E, 5, 6 $\beta$ -EC and CT uptake respectively (Fig. 5A-D). We next found that in the absence of FBS, which provides lipids including cholesterol to cells,

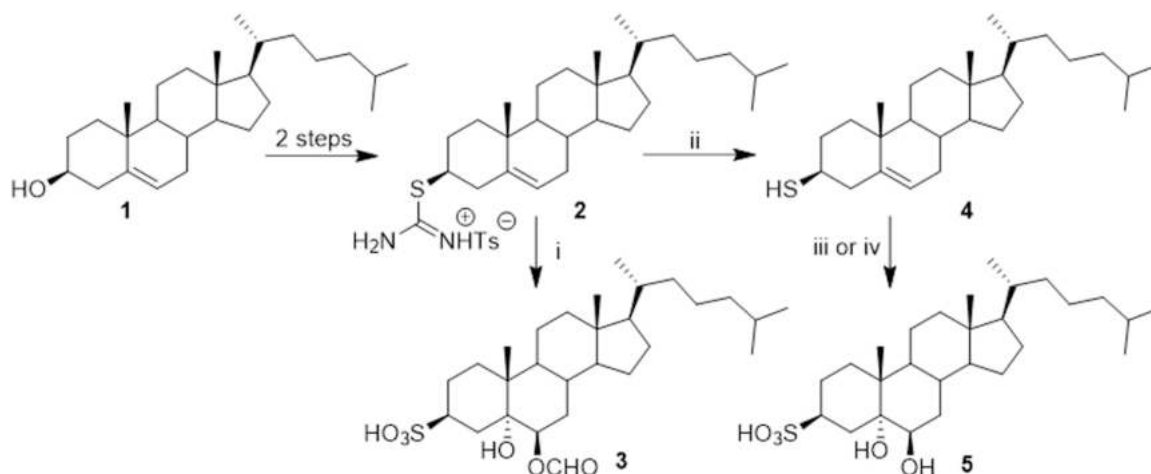


**Fig. 2.** Chemical synthesis of CDSN. i:  $\text{HCOOH}$ ,  $\text{H}_2\text{O}_2$ , 50 °C, 1 h. ii: 3 equiv NaOH, EtOH, reflux, 2 h, 86%. iii: a:  $\text{HCOOH}$ ,  $\text{H}_2\text{O}_2$ ,  $\text{CH}_2\text{Cl}_2$ , 0 °C- rt, 24 h. b: MeOH, 60 °C, 1 h, 92%. iv: a:  $\text{HCOOH}$ ,  $\text{H}_2\text{O}_2$ , THF, 0 °C-rt 1 h, 50–60 °C, 3 h, rt, 24 h. b: MeOH, 60 °C, 1 h, 95%.



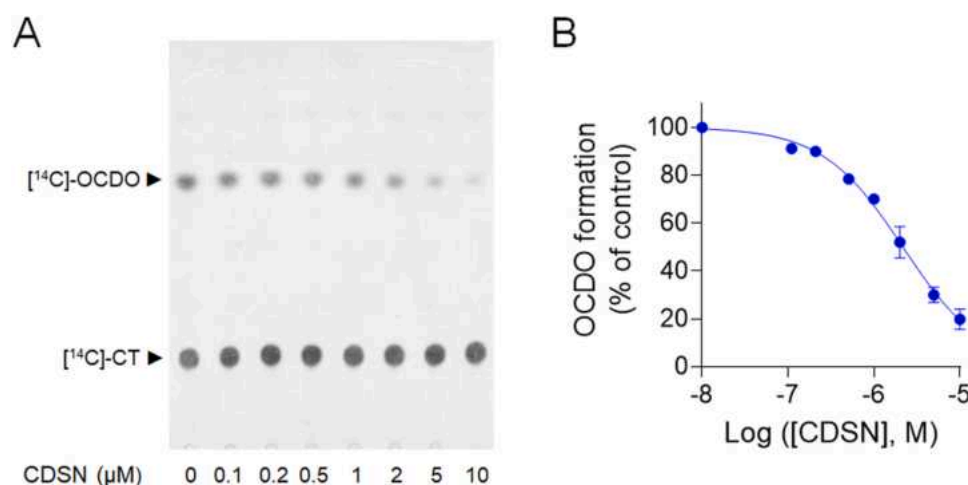


**Fig. 3.** Effect of CDSN on OCDO biosynthesis. HEK293T-11HSD2 cells lysate (20 μg) were incubated with 1 μM of [<sup>14</sup>C]-CT at 37 °C for 10 min with increasing concentrations of CDSN ranging from 1 to 10 μM. OCDO biosynthesis was assayed by measuring the conversion of [<sup>14</sup>C]-CT to [<sup>14</sup>C]-OCDO by thin-layer chromatography (TLC) and quantified as described in Materials and Methods. A) On the left panel, a representative autoradiogram of a dose-dependent inhibition of OCDO production by CDSN in HEK293T-11HSD2 cells lysate. B) on the right panel, quantification of the dose-dependent inhibition of OCDO biosynthesis activity measured by TLC with increasing concentrations of CDSN. Values are the mean ± S.E. of three independent experiments each carried out in duplicate.

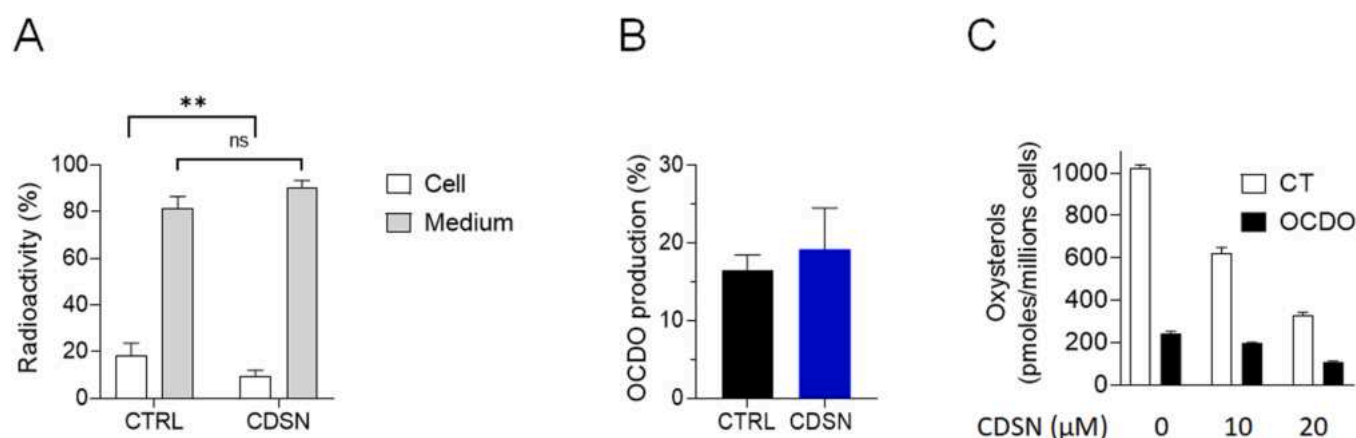


**Fig. 4.** Measurement of the impact of CDSN on [<sup>14</sup>C]-CT uptake and metabolism in MCF-7 cells. MCF-7 cells were incubated with 1 μM of [<sup>14</sup>C]-CT for 5 h with or without 20 μM of CDSN. 11β-HSD2 activity (OCDO synthase) was assayed by measuring the conversion of [<sup>14</sup>C]-CT to [<sup>14</sup>C]-OCDO by TLC and quantified as described in Materials and Methods. (A) Quantification of intracellular radioactivity from lipidic extracts of MCF-7 treated with solvent vehicle and CDSN (20 μM); (B) Percentage of intracellular conversion of [<sup>14</sup>C]-CT into [<sup>14</sup>C]-OCDO on MCF-7 treated with solvent vehicle and CDSN (20 μM); (C) Quantification of the intracellular level of [<sup>14</sup>C]-CT and [<sup>14</sup>C]-oncosterone on MCF-7 treated with solvent vehicle or 20 μM CDSN. Values are the mean ± S.E. of three independent experiments each carried out in duplicate. Statistical analysis was carried out using a Student's t-test for unpaired variables. \*, \*\* and \*\*\* in the figures refer to statistical probabilities (P) of < 0.05, < 0.01 and < 0.001, respectively, compared with control cells that received solvent vehicle alone.

CDSN totally blocked sterols uptake suggesting that added sterols are uptaken by cells when associated to FBS components such as lipoproteins. In conclusion, we show that CDSN is an inhibitor of CT, 5,6α-E, 5, 6β-EC and cholesterol uptake in MCF-7 cells, while Ez is slightly active to block only cholesterol uptake. These data suggest that the control by CDSN of the uptake of these sterols is independent of NPC1L1 and may be required for the LDLR endocytic pathway.

### 3.5. Effect CDSN alone or in combination with post-lanosterol cholesterol biosynthesis inhibitors on MCF-7 cells proliferation and viability

We report here that CDSN inhibits MCF-7 proliferation but was not cytotoxic up to 20 μM (Fig. 6A-C). We previously reported that tamoxifen (Tam) and PBPE triggered the inhibition of cholesterol biosynthesis and a massive accumulation of free sterols [39,64–68]. This was characterized at the cellular level by an increased of the vesicular filipin staining associated to the presence of multilamellar bodies (MLB) in the cytoplasm of MCF-7 cells [39,64–68]. Since the endocytic LDLR pathway is involved NPC1 transporters [69], we were interested to determine if CDSN could enhance sterol storage in MCF-7 cells. Cells were exposed to Tam, PBPE with or without CDSN for 72 h and then cell proliferation and viability was measured. We observed that single

treatment with Tam or PBPE inhibit cell proliferation but not viability at these concentrations. We observed that the combination of CDSN with Tam or PBPE induce anoikis that was not observed with single treatment (Fig. 6A) and affect drastically cell viability (Fig. 6C). These data show that CDSN inhibits MCF-7 cell proliferation and this effect was potentiated by the inhibitors of cholesterol biosynthesis Tam and PBPE which led to anoikis and massive cell death.

### 3.6. The combination of CDSN with Tam and PBPE induces free sterol accumulation and the appearance of giant multilamellar bodies

We next investigated the impact of CDSN treatment of MCF-7 cells on intracellular sterol accumulation, filipin labeling and MLB formation. CDSN alone does not trigger an increased filipin labeling or the appearance of MLB. Tam or PBPE alone trigger an increase of filipin labeling (Fig. 7A) confirming previously published observations [64, 65]. As expected, combination treatments of MCF-7 cells led to an increased filipin labeling (Fig. 7B) and the accumulation of MLB (Fig. 8). These data show that CDSN impact on the dynamic of sterol homeostasis in MCF-7 possibly involving NPC1.

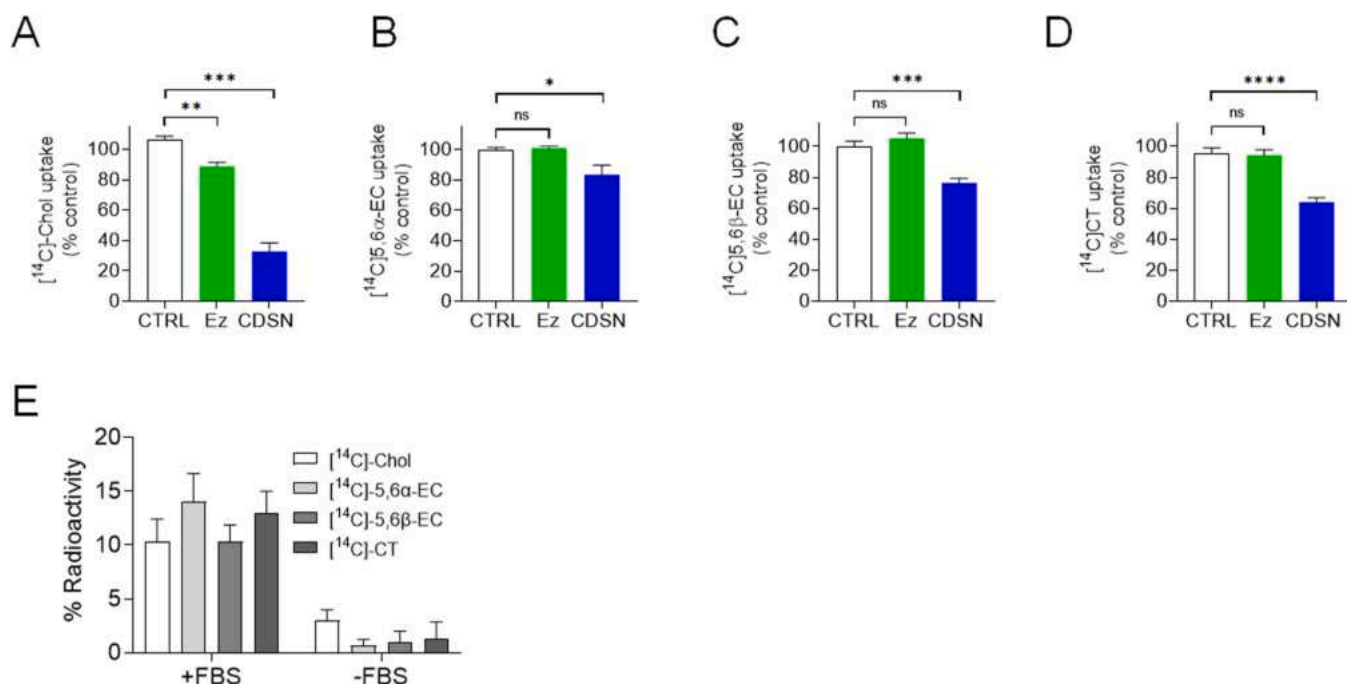


**Fig. 5.** MCF-7 cells were incubated with 1  $\mu$ M of [<sup>14</sup>C]-cholesterol, 1  $\mu$ M of [<sup>14</sup>C]- 5,6 $\alpha$ -EC, 1  $\mu$ M of [<sup>14</sup>C]- 5,6 $\beta$ -EC or 1  $\mu$ M of [<sup>14</sup>C]-CT for 5 h with or without 40  $\mu$ M of ezetimibe, or 20  $\mu$ M of CDSN. Cells were lysed with 0.1% SDS and intracellular radioactivity counted with a  $\beta$ -counter. Quantification of intracellular radioactivity from MCF-7 cells exposed to [<sup>14</sup>C]-Cholesterol (A), [<sup>14</sup>C]- 5,6 $\alpha$ -EC (B), [<sup>14</sup>C]- 5,6 $\beta$ -EC (C) and [<sup>14</sup>C]-CT (D). The intracellular radioactivity was expressed as the percentage of the intracellular radioactivity measured in the absence of tested compounds (control with solvent vehicle). Values are the mean  $\pm$  S.E. of three independent experiments each carried out in duplicate. Statistical analyses were carried out using a Student's t-test for unpaired variables. \*, \*\* and \*\*\* in the figures refer to statistical probabilities (P) of < 0.05, < 0.01 and < 0.001, respectively, compared with control cells that received solvent vehicle alone.

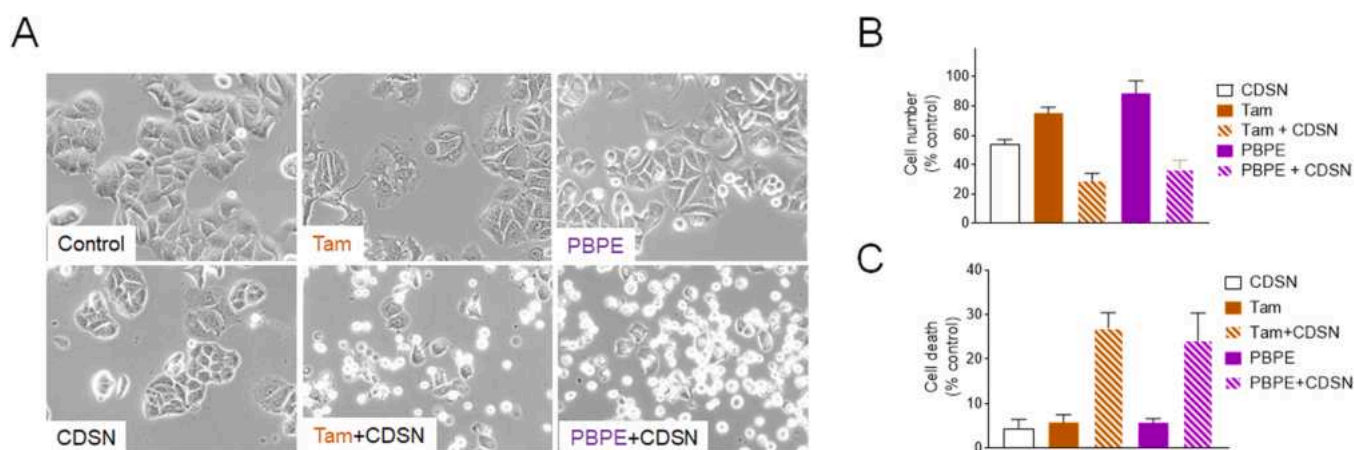


**Fig. 6.** Effect CDSN on MCF-7 cells proliferation and viability. MCF-7 cells were exposed for 3 days to solvent vehicle (Control), 10  $\mu$ M CDSN alone or a combination with 2.5  $\mu$ M Tam, or 10  $\mu$ M PBPE. A) Morphological changes observed by light microscopy (x40); B) Antiproliferative activity. Cells were harvested by trypsinization and counted on a Malassez chamber. Data were expressed as the percentage of cell number relative to control cells; C) Cell death measurement. Cell death was determined by Trypan blue exclusion test. Data were expressed as the percentage of cell death relative to control cells. Values are the mean  $\pm$  S.E. of three independent experiments each carried out in duplicate. Statistical analysis was carried out using a Student's t-test for unpaired variables. \*, \*\* and \*\*\* in the figures refer to statistical probabilities (P) of < 0.05, < 0.01 and < 0.001, respectively, compared with control cells that received solvent vehicle alone.

#### 4. Conclusion

We report herein the chemical synthesis of CDSN as a non-hydrolysable analogue of CTS. The synthesis is original and gives the product of interest in 1 step from thiocholesterol oxidation with peroxyformic acid with a yield of 92 % and 95 % when using  $\text{CH}_2\text{Cl}_2$  or THF respectively as solvents for the reaction. We next evaluate the biological properties of CDSN, which is a non-hydrolysable analogue of CTS. We first look at the impact of CDSN on the transformation of CT into oncosterone and found that it is a potent inhibitor of the enzyme in cell

lyzates, suggesting it could be a substrate or an endogenous inhibitor of the oncosterone synthase (11 $\beta$ -HSD2) (Fig. 9A-B). While we observed that the oncosterone (OCDO) level decreased drastically under CDSN treatment, a careful analysis of this effect ruled out an inhibition of the oncosterone synthase in that case because we found that CDSN inhibited drastically the uptake of CT by MCF-7 cells. In addition, we found that CDSN inhibited not only the uptake of CT but also the uptake of cholesterol, 5,6 $\alpha$ -EC and 5,6 $\beta$ -EC. These data suggest that exogenous CTS could control 5,6-EC and CT homeostasis. The uptake of these sterols can be mediated through several mechanisms using the endocytic

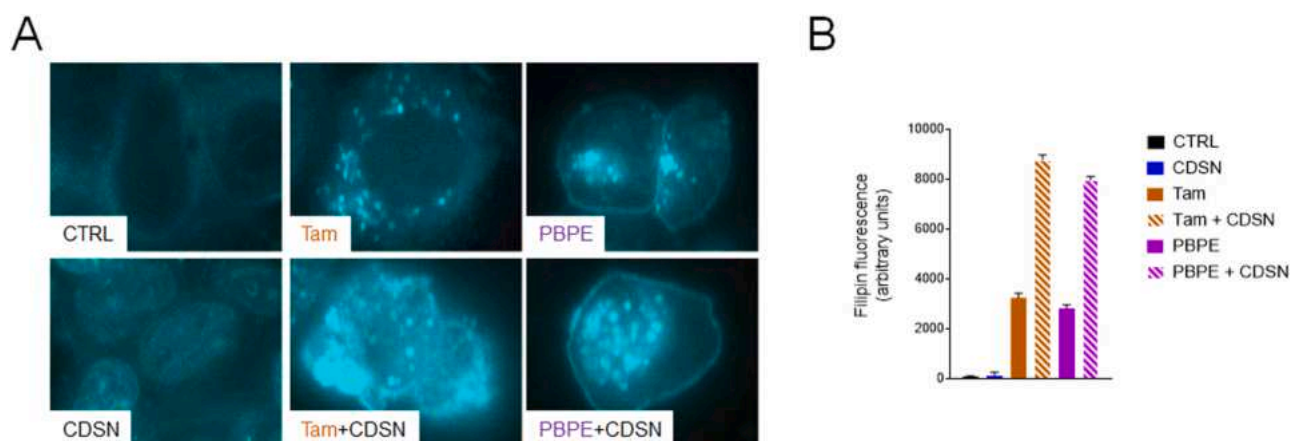


**Fig. 7.** Representative pictures of cells stained with filipin and analyzed by fluorescent microscopy, magnification x 40. MCF-7 cells were exposed for 2 days to solvent vehicle (CTRL); Tam (2.5  $\mu$ M) PBPE (10  $\mu$ M), CDSN (10  $\mu$ M) or a combination of Tam (2.5  $\mu$ M) or PBPE (10  $\mu$ M) with CDSN (10  $\mu$ M).

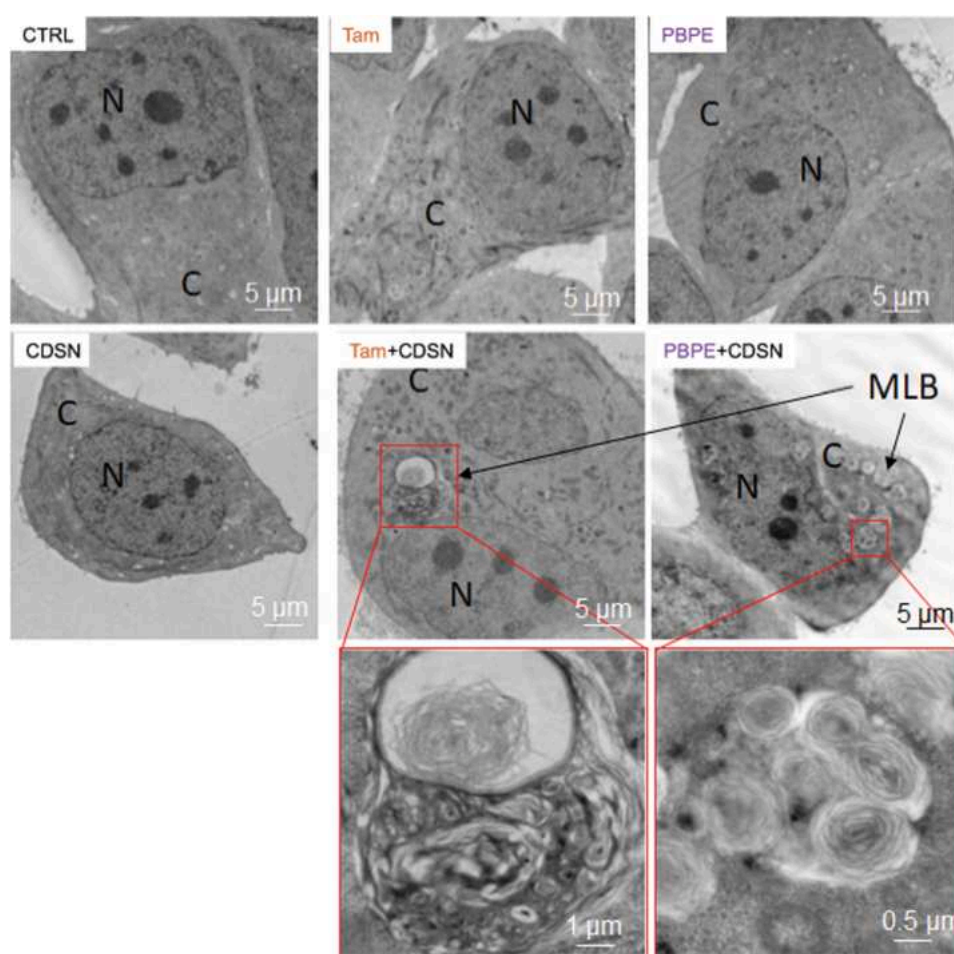


**Fig. 8.** Transmission electron microscopic ultrastructural analysis of MCF7 cells exposed for 2 days to solvent vehicle (CTRL); Tam (2.5  $\mu$ M) PBPE (10  $\mu$ M), CDSN (10  $\mu$ M) or a combination of Tam (2.5  $\mu$ M) and PBPE (10  $\mu$ M) with CDSN (10  $\mu$ M). N, nucleus; C, cytoplasm; LD, lipid droplet; MLB, multilamellar bodies. Experiments were repeated at least three times in duplicate with comparable results. The images presented are representative of three independent experiments.

pathway via the LDLR [70], or transporters such as NPC1L1 which is expressed in MCF-7 cells [71]. We found that CDSN reduces the uptake of cholesterol, which can be partly inhibited by Ezetimide, suggesting that NPC1L1 control the uptake of 20% of cholesterol in MCF-7 cells. Ezetimide was inefficient to block the uptake of CT and 5,6-ECs suggesting that another mechanism was required. On the other hand, we found that FBS was required for the uptake of sterols suggesting that the tested

sterols were taken up by cells via lipoproteins such as low density lipoproteins (LDL). LDL are taken up by cells via LDL receptor, which is controlled by NPC1 [69]. NPC1 is a transporter involved in the transport of cholesterol from the reticulum endoplasmic to lysosomes. It is also involved in the clathrin-coated pits endocytic pathway controlling lipoproteins and virus uptake, which led to the development of NPC1 inhibitors. NPC1 has been identified as pharmacological targets that can



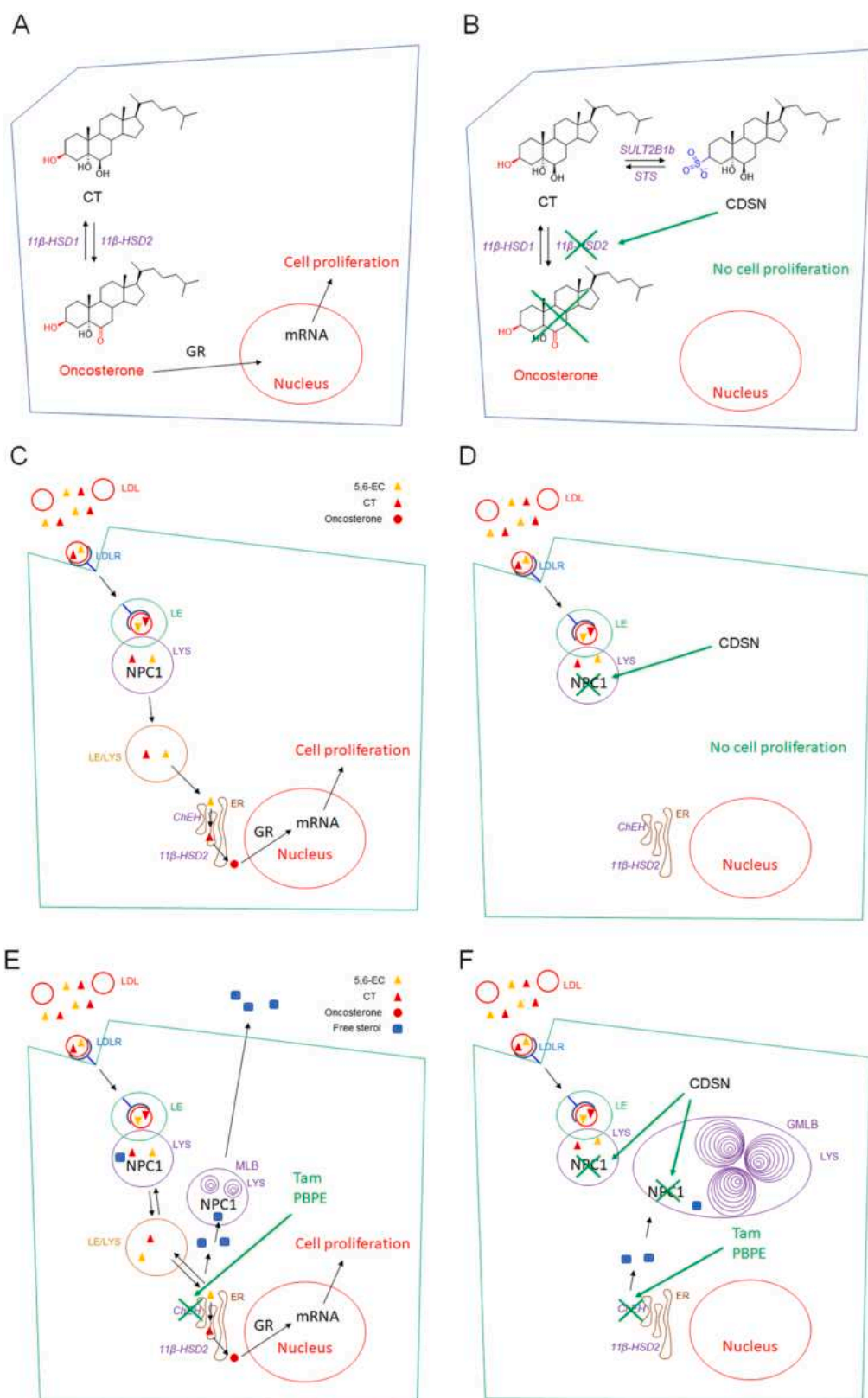


**Fig. 9.** (A) Biosynthesis of oncosterone from CT and stimulation of cell proliferation through the activation of GR by oncosterone. (B) CDSN inhibits the biosynthesis of oncosterone at the 11β-HSD2 level and cell proliferation. (C) LDL transport 5,6-EC and CT into cells that can be further metabolized into oncosterone, which stimulates cell proliferation via the activation of GR. (D) CDSN inhibits 5,6-EC and CT uptake by blocking NPC1, and thus inhibiting oncosterone production and cell proliferation. (E) Tamoxifen and PBE inhibit the ChEH/EBP complex which blocks oncosterone biosynthesis and induce free sterols accumulation due to EBP inhibition. Free sterols accumulation led to the appearance of MLB. (F) Co-treatment of Tam or PBE with CDSN led to the overaccumulation of free sterols into giant MLB. GR: glucocorticoid receptor; LDL: low density lipoproteins; LDLR: LDL receptor; LE: late endosomes; LYS: lysosomes; ER: endoplasmic reticulum; MLB: multilamellar bodies; GMLB: giant MLB.



block the host cell entrance and the infectivity of several viruses such as ebola virus [72–74], bluetongue virus [75], reovirus [76], african swine fever virus [77], flovovirus [78], HIV [79] and SARS-Cov-2 [80,81]. Interestingly, CT was also used as a chemotype for the development of inhibitors of NPC1 transporters [82,83]. These data support that CDSN inhibits NPC1 and the uptake of 5,6-EC and CT complexed with LDL as summarized on Fig. 9C-D.

CDSN inhibits cell proliferation but was found weakly cytotoxic. The fact that NPC1 may control the uptake of sterols of interest led us test compounds that are inhibitors of cholesterol biosynthesis and that induced the accumulation of free sterols, to determine if CDSN amplified or not sterol accumulation. Tam and PBE have been shown to induce the accumulation of sterols due to their inhibition of cholesterologenic enzymes [64–68,84]. This accumulation was associated to the induction of autophagy in MCF-7 cells and to the appearance of MLB in the cytoplasm of cells [47]. Tam or PBPE combination treatment with CDSN of MCF-7 cells induce the appearance of giant MLB that may results from the inhibition of sterol trafficking in these cells (Fig. 9E-F). The accumulation of sterols and the presence of MLB recapitulates ultrastructural modifications reported in Type C Niemann-Pick disease fibroblasts [85,86].

Altogether, our data strongly suggest that CDSN and therefore CDS could display antitumor activity on breast cancer through the inhibition of oncosterone production. This latter could arise through two mechanisms: 1°) the inhibition of oncosterone biosynthesis by intracellular CDS (Figs. 9A-B) and 2°) the inhibition of cellular uptake of oncosterone precursors (5,6-EC and CT) by extracellular CDS (Fig. 9C-D). This strongly suggests that CDS is a natural CT metabolite that can regulate oncosterone biosynthesis and LDLR-mediated oxysterol cellular uptake.

The impact of CDSN in combination with Tam, PBPE in vivo on tumor implanted in mice would be necessary to validate the potential therapeutic interest of CDSN for BC treatment and suggests that the endogenous production of CTS by BC cells could represent an predictive factor of sensitivity to hormonotherapy with tamoxifen and eventually other SERMs. The impact of combination treatments on other BC cells with various phenotypes in term of cholesterol/oxysterols homeostasis, biosynthesis, metabolism, and sterol receptor is worthy of investigation. In particular, BC cell lines that are representative of the different BC subtypes in vitro and in vivo deserves further investigations. These studies would help to determine if CDSN could be a specific or general tool with a therapeutic potential and would paved the way for exploring the importance of the CDS pathway in the physio-pathology and in anticancer strategies.

The potential role of CDS on different pathologies such as Niemann-Pick Type C disease, viral infection and cancer deserves further investigation.

#### CRedit authorship contribution statement

**Philippe de Medina:** original draft; experimental, radiolabelled chemistry, biochemistry, cell biology, writing, review. **Silia Ayadi:** experimental, radiolabelled chemistry, biochemistry, cell biology, writing, review. **Régis Soulès:** radiolabelled chemistry, writing. **Bruno Payre:** TEM, writing. **Sandrine Rup-Jacques:** Chemistry, structure analysis; writing, review. **Mohammad Samadi:** original draft, chemistry, structure analysis; writing, review. **Sandrine Silvente-Poirot:** original draft; writing, review. **Marc Poirot:** Conceptualization, original draft; writing, review.

#### Declaration of Competing Interest

The authors declare no conflict of interest.

#### Data availability

Data will be made available on request.

#### Acknowledgments

This work was funded by an internal grant from the “Institut National de la Santé et de la Recherche Médicale”, the “Université de Toulouse III”, the “Agence Nationale de la Recherche” (DASYNT2, ANR-20-CE11-0005) and the Institut National du Cancer (PLBIO-2018-145). This study has been partially supported through the grant EUR CARE N°ANR-18-EURE-0003 in the framework of the Program des Investissements d’Avenir.

#### Appendix A. Supporting information

Supplementary data associated with this article can be found in the online version at doi:10.1016/j.jsbmb.2023.106396.

#### References

- [1] P. de Medina, S. Silvente-Poirot, M. Poirot, Oxysterols are potential physiological regulators of ageing, *Ageing Res. Rev.* 77 (2022), 101615.
- [2] M. Poirot, S. Silvente-Poirot, m. Team Cholesterol, i. therapeutic, Oxysterols: An expanding family of structurally diversified bioactive steroids, *J. Steroid Biochem. Mol. Biol.* 194 (2019), 105443.
- [3] P. de Medina, K. Diallo, E. Huc-Claustre, M. Attia, R. Soules, S. Silvente-Poirot, M. Poirot, The 5,6-epoxycholesterol metabolic pathway in breast cancer: emergence of new pharmacological targets, *Br. J. Pharmacol.* 178 (16) (2021) 3248–3260.
- [4] S. Silvente-Poirot, F. Dalenc, M. Poirot, The effects of cholesterol-derived oncometabolites on nuclear receptor function in cancer, *Cancer Res.* 78 (17) (2018) 4803–4808.
- [5] D.J. Kojetin, T.P. Burris, REV-ERB and ROR nuclear receptors as drug targets, *Nat. Rev. Drug Discov.* 13 (3) (2014) 197–216.
- [6] B.A. Janowski, M.J. Grogan, S.A. Jones, G.B. Wisely, S.A. Kliewer, E.J. Corey, D. J. Mangelsdorf, Structural requirements of ligands for the oxysterol liver X receptors LXRA and LXRbeta, *Proc. Natl. Acad. Sci. USA* 96 (1) (1999) 266–271.
- [7] V. Daggubati, D.R. Raleigh, N. Sever, Sterol regulation of developmental and oncogenic Hedgehog signaling, *Biochem. Pharmacol.* 196 (2022), 114647.
- [8] N. Sever, R.K. Mann, L. Xu, W.J. Snell, C.I. Hernandez-Lara, N.A. Porter, P. A. Beachy, Endogenous B-ring oxysterols inhibit the Hedgehog component smoothened in a manner distinct from cyclopamine or side-chain oxysterols, *Proc. Natl. Acad. Sci. USA* 113 (21) (2016) 5904–5909.
- [9] L. Raccosta, R. Fontana, D. Maggioni, C. Lanterna, E.J. Villablanca, A. Paniccia, A. Musumeci, E. Chiricozzi, M.L. Trincavelli, S. Daniele, C. Martini, J. A. Gustafsson, C. Doglioni, S.G. Feo, A. Leiva, M.G. Ciampa, L. Mauri, C. Sensi, A. Prinetti, I. Eberini, J.R. Mora, C. Bordignon, K.R. Steffensen, S. Sonnino, S. Sozzani, C. Traversari, V. Russo, The oxysterol-CXCR2 axis plays a key role in the recruitment of tumor-promoting neutrophils, *J. Exp. Med.* 210 (9) (2013) 1711–1728.
- [10] S. Nachtergaele, L.K. Mydock, K. Krishnan, J. Rammohan, P.H. Schlesinger, D. F. Covey, R. Rohatgi, Oxysterols are allosteric activators of the oncoprotein Smoothened, *Nat. Chem. Biol.* 8 (2) (2012) 211–220.
- [11] S. Hannedouche, J. Zhang, T. Yi, W. Shen, D. Nguyen, J.P. Pereira, D. Guerini, B. U. Baumgarten, S. Roggo, B. Wen, R. Knochenmuss, S. Noel, F. Gessier, L.M. Kelly, M. Vanek, S. Laurent, I. Preuss, C. Miault, I. Christen, R. Karuna, W. Li, D.I. Koo, T. Suply, C. Schmedt, E.C. Peters, R. Falchetto, A. Katopodis, C. Spanka, M.O. Roy, M. Dethieux, Y.A. Chen, P.G. Schultz, C.Y. Cho, K. Seuwen, J.G. Cyster, A.W. Sailer, Oxysterols direct immune cell migration via EBI2, *Nature* 475 (7357) (2011) 524–527.
- [12] M.A. Rogers, J. Liu, B.L. Song, B.L. Li, C.C. Chang, T.Y. Chang, Acyl-CoA: cholesterol acyltransferases (ACATs/SOATs): enzymes with multiple sterols as substrates and as activators, *J. Steroid Biochem. Mol. Biol.* 151 (2015) 102–107.
- [13] S. Silvente-Poirot, M. Poirot, Cholesterol epoxide hydrolase and cancer, *Curr. Opin. Pharmacol.* 12 (6) (2012) 696–703.
- [14] P. de Medina, M.R. Paillasse, G. Segala, M. Poirot, S. Silvente-Poirot, Identification and pharmacological characterization of cholesterol-5,6-epoxide hydrolase as a target for tamoxifen and AEBs ligands, *Proc. Natl. Acad. Sci. USA* 107 (30) (2010) 13520–13525.
- [15] G.J. Schroeffer Jr., Oxysterols: modulators of cholesterol metabolism and other processes, *Physiol. Rev.* 80 (1) (2000) 361–554.
- [16] R.E. Infante, L. Abi-Mosleh, A. Radhakrishnan, J.D. Dale, M.S. Brown, J. L. Goldstein, Purified NPC1 protein. I. Binding of cholesterol and oxysterols to a 1278-amino acid membrane protein, *J. Biol. Chem.* 283 (2) (2008) 1052–1063.
- [17] R.E. Infante, A. Radhakrishnan, L. Abi-Mosleh, L.N. Kinch, M.L. Wang, N. V. Grishin, J.L. Goldstein, M.S. Brown, Purified NPC1 protein: II. Localization of sterol binding to a 240-amino acid soluble luminal loop, *J. Biol. Chem.* 283 (2) (2008) 1064–1075.
- [18] V.M. Olkkonen, The emerging roles of OSBP-related proteins in cancer: impacts through phosphoinositide metabolism and protein-protein interactions, *Biochem. Pharmacol.* 196 (2022), 114455.
- [19] A. Radhakrishnan, Y. Ikeda, H.J. Kwon, M.S. Brown, J.L. Goldstein, Sterol-regulated transport of SREBPs from endoplasmic reticulum to Golgi: oxysterols

- block transport by binding to Insig, *Proc. Natl. Acad. Sci. USA* 104 (16) (2007) 6511–6518.
- [20] L. Reinmuth, C.-C. Hsiao, J. Hamann, M. Rosenkilde, J. Mackrill, Multiple targets for oxysterols in their regulation of the immune system, *Cells* (2021).
- [21] J.H. Zhang, L. Ge, W. Qi, L. Zhang, H.H. Miao, B.L. Li, M. Yang, B.L. Song, The N-terminal domain of NPC1L1 protein binds cholesterol and plays essential roles in cholesterol uptake, *J. Biol. Chem.* 286 (28) (2011) 25088–25097.
- [22] M. Poirot, R. Soules, A. Mallinger, F. Dalenc, S. Silvente-Poirot, Chemistry, biochemistry, metabolic fate and mechanism of action of 6-oxo-cholestan-3beta,5alpha-diol (OCDO), a tumor promoter and cholesterol metabolite, *Biochimie* 153 (2018) 139–149.
- [23] M. Poirot, S. Silvente-Poirot, Cholesterol-5,6-epoxides: chemistry, biochemistry, metabolic fate and cancer, *Biochimie* 95 (3) (2013) 622–631.
- [24] B.N. Zanjani, A. Samadi, S.Y. Isikhan, I. Lay, S. Beyaz, A. Gelincik, S. Buyukozturk, N. Arda, Plasma levels of oxysterols 7-ketocholesterol and cholestane-3beta, 5alpha, 6beta-triol in patients with allergic asthma, *J. Asthma* 60 (2) (2023) 288–297.
- [25] A.N. Dang, D. J. Chang, X. Jiang, L.A. Wolfe, B.G. Ng, C. Lam, R.E. Schnur, K. Allis, H. Hansikova, N. Ondruskova, S.D. O'Connor, A. Sanchez-Valle, A. Vollo, R.Y. Wang, Z. Wolfenson, J. Perreault, D.S. Ory, H.H. Freeze, J.L. Merritt, F. D. Porter, Elevated oxysterol and N-palmitoyl-O-phosphocholineserine levels in congenital disorders of glycosylation, *J. Inherit. Metab. Dis.* 46 (2) (2023) 326–334.
- [26] F.D. Porter, D.E. Scherrer, M.H. Lanier, S.J. Langmade, V. Molugu, S.E. Gale, D. Olzeski, R. Sidhu, D.J. Dietzen, R. Fu, C.A. Wassif, N.M. Yanjanin, S.P. Marso, J. House, C. Vite, J.E. Schaffer, D.S. Ory, Cholesterol oxidation products are sensitive and specific blood-based biomarkers for Niemann-Pick C1 disease, *Sci. Transl. Med.* 2 (56) (2010), 56ra81.
- [27] M. Messedi, W. Guidara, S. Grayaa, W. Khrouf, M. Snoussi, Z. Bahloul, D. Bonnefont-Rousselot, F. Lamari, F. Ayadi, Selected plasma oxysterols as a potential multi-marker biosignature panel for Behcet's Disease, *J. Steroid Biochem. Mol. Biol.* 221 (2022), 106122.
- [28] W. Guidara, M. Messedi, M. Naifar, M. Maalej, W. Khrouf, S. Grayaa, M. Maalej, D. Bonnefont-Rousselot, F. Lamari, F. Ayadi, Plasma oxysterols in drug-free patients with schizophrenia, *J. Steroid Biochem. Mol. Biol.* 221 (2022), 106123.
- [29] W. Guidara, M. Messedi, M. Maalej, M. Naifar, W. Khrouf, S. Grayaa, M. Maalej, D. Bonnefont-Rousselot, F. Lamari, F. Ayadi, Plasma oxysterols: Altered level of plasma 24-hydroxycholesterol in patients with bipolar disorder, *J. Steroid Biochem. Mol. Biol.* 211 (2021), 105902.
- [30] A. Kloudova-Spalenkova, Y.F. Ueng, S. Wei, K. Kopeckova, F. Peter Guengerich, P. Soucek, Plasma oxysterol levels in luminal subtype breast cancer patients are associated with clinical data, *J. Steroid Biochem. Mol. Biol.* 197 (2020), 105566.
- [31] S. Boenzi, F. Deodato, R. Taurisano, B.M. Goffredo, C. Rizzo, C. Dionisi-Vici, Evaluation of plasma cholestane-3beta,5alpha,6beta-triol and 7-ketocholesterol in inherited disorders related to cholesterol metabolism, *J. Lipid Res.* 57 (3) (2016) 361–367.
- [32] Y.W. Cheng, J.J. Kang, Y.L. Shih, Y.L. Lo, C.F. Wang, Cholesterol-3-beta, 5-alpha, 6-beta-triol induced genotoxicity through reactive oxygen species formation, *Food Chem. Toxicol.* 43 (4) (2005) 617–622.
- [33] H. Liu, L. Yuan, S. Xu, T. Zhang, K. Wang, Cholestane-3beta, 5alpha, 6beta-triol promotes vascular smooth muscle cells calcification, *Life Sci.* 76 (5) (2004) 533–543.
- [34] L. Tang, Y. Wang, T. Leng, H. Sun, Y. Zhou, W. Zhu, P. Qiu, J. Zhang, B. Lu, M. Yan, W. Chen, X. Su, W. Yin, Y. Huang, H. Hu, G. Yan, Cholesterol metabolite cholestane-3beta,5alpha,6beta-triol suppresses epileptic seizures by negative modulation of voltage-gated sodium channels, *Steroids* 98 (2015) 166–172.
- [35] H. Hu, Y. Zhou, T. Leng, A. Liu, Y. Wang, X. You, J. Chen, L. Tang, W. Chen, P. Qiu, W. Yin, Y. Huang, J. Zhang, L. Wang, H. Sang, G. Yan, The major cholesterol metabolite cholestane-3beta,5alpha,6beta-triol functions as an endogenous neuroprotectant, *J. Neurosci.* 34 (34) (2014) 11426–11438.
- [36] M.R. Paillasse, N. Saffon, H. Gornitzka, S. Silvente-Poirot, M. Poirot, P. de Medina, Surprising unreactivity of cholesterol-5,6-epoxides towards nucleophiles, *J. Lipid Res.* 53 (4) (2012) 718–725.
- [37] M. Voisin, P. de Medina, A. Mallinger, F. Dalenc, E. Huc-Claustre, J. Leignadier, N. Serhan, R. Soules, G. Segala, A. Mougler, E. Noguier, L. Mhamdi, E. Bacquie, L. Iuliano, C. Zerbinati, M. Lacroix-Triki, L. Chaltiel, T. Filleron, V. Cavaillès, T. Al Saati, P. Rochaix, R. Duprez-Paumier, C. Franchet, L. Ligat, F. Lopez, M. Record, M. Poirot, S. Silvente-Poirot, Identification of a tumor-promoter cholesterol metabolite in human breast cancers acting through the glucocorticoid receptor, *Proc. Natl. Acad. Sci. USA* 114 (44) (2017) E9346–E9355.
- [38] X.W. Ji, T.Y. Zhou, Y. Lu, M.J. Wei, W. Lu, W.C. Cho, Breast cancer treatment and sulfotransferase, *Expert Opin. Ther. Targets* 19 (6) (2015) 821–834.
- [39] G. Segala, P. de Medina, L. Iuliano, C. Zerbinati, M.R. Paillasse, E. Noguier, F. Dalenc, B. Payre, V.C. Jordan, M. Record, S. Silvente-Poirot, M. Poirot, 5,6-Epoxy-cholesterols contribute to the anticancer pharmacology of tamoxifen in breast cancer cells, *Biochem. Pharmacol.* 86 (1) (2013) 175–189.
- [40] H. Fuda, N.B. Javitt, K. Mitamura, S. Ikegawa, C.A. Strott, Oxysterols are substrates for cholesterol sulfotransferase, *J. Lipid Res.* 48 (6) (2007) 1343–1352.
- [41] S.J. Bensinger, M.N. Bradley, S.B. Joseph, N. Zelcer, E.M. Janssen, M.A. Hausner, R. Shih, J.S. Parks, P.A. Edwards, B.D. Jamieson, P. Tontonoz, LXR signaling couples sterol metabolism to proliferation in the acquired immune response, *Cell* 134 (1) (2008) 97–111.
- [42] J.W. Mueller, L.C. Gilligan, J. Idkowiak, W. Arlt, P.A. Foster, The regulation of steroid action by sulfation and desulfation, *Endocr. Rev.* 36 (5) (2015) 526–563.
- [43] O. Hanyu, H. Nakae, T. Miida, Y. Higashi, H. Fuda, M. Endo, A. Kohjitani, H. Sone, C.A. Strott, Cholesterol sulfate induces expression of the skin barrier protein filaggrin in normal human epidermal keratinocytes through induction of RORalpha, *Biochem. Biophys. Res. Commun.* 428 (1) (2012) 99–104.
- [44] T. Tatsuguchi, T. Uruno, Y. Sugiura, D. Sakata, Y. Izumi, T. Sakurai, Y. Hattori, E. Oki, N. Kubota, K. Nishimoto, M. Oyama, K. Kunimura, T. Ohki, T. Bamba, H. Tahara, M. Sakamoto, M. Nakamura, M. Suematsu, Y. Fukui, Cancer-derived cholesterol sulfate is a key mediator to prevent tumor infiltration by effector T cells, *Int. Immunol.* 34 (5) (2022) 277–289.
- [45] X. Zhang, Q. Bai, G. Kakiyama, L. Xu, J.K. Kim, W.M. Pandak Jr., S. Ren, Cholesterol metabolite, 5-cholesten-3beta-25-diol-3-sulfate, promotes hepatic proliferation in mice, *J. Steroid Biochem. Mol. Biol.* 132 (3–5) (2012) 262–270.
- [46] C. Song, R.A. Hiipakka, S. Liao, Auto-oxidized cholesterol sulfates are antagonistic ligands of liver X receptors: implications for the development and treatment of atherosclerosis, *Steroids* 66 (6) (2001) 473–479.
- [47] J. Leignadier, F. Dalenc, M. Poirot, S. Silvente-Poirot, Improving the efficacy of hormone therapy in breast cancer: the role of cholesterol metabolism in SERM-mediated autophagy, cell differentiation and death, *Biochem Pharmacol.* 144 (2017) 18–28.
- [48] Y. Wang, W. Lin, J.E. Brown, L. Chen, W.M. Pandak, P.B. Hylemon, S. Ren, 25-Hydroxycholesterol 3-sulfate is an endogenous ligand of DNA methyltransferases in hepatocytes, *J. Lipid Res.* 62 (2021), 100063.
- [49] Y. Wang, X. Li, S. Ren, Cholesterol metabolites 25-hydroxycholesterol and 25-hydroxycholesterol 3-sulfate are potent negative regulators: from discovery to clinical usage, *Metabolites* 11 (1) (2020).
- [50] Y. Wang, L. Chen, W.M. Pandak, D. Heuman, P.B. Hylemon, S. Ren, High glucose induces lipid accumulation via 25-hydroxycholesterol DNA-CpG methylation, *iScience* 23 (5) (2020), 101102.
- [51] E.J. Villablanca, L. Raccosta, D. Zhou, R. Fontana, D. Maggioni, A. Negro, F. Sanvito, M. Ponzoni, B. Valentini, M. Bregni, A. Prinetti, K.R. Steffensen, S. Sonnino, J.A. Gustafsson, C. Dogliani, C. Bordignon, C. Traversari, V. Russo, Tumor-mediated liver X receptor-alpha activation inhibits CC chemokine receptor-7 expression on dendritic cells and dampens antitumor responses, *Nat. Med.* 16 (1) (2010) 98–105.
- [52] L.D. Sanchez, L. Pontini, M. Marinozzi, L.C. Sanchez-Aranguren, A. Reis, I.H. K. Dias, Cholesterol and oxysterol sulfates: pathophysiological roles and analytical challenges, *Br. J. Pharmacol.* 178 (16) (2021) 3327–3341.
- [53] P.K. Li, R. Pillai, B.L. Young, W.H. Bender, D.M. Martino, F.T. Lin, Synthesis and biochemical studies of estrone sulfatase inhibitors, *Steroids* 58 (3) (1993) 106–111.
- [54] M. Poirot, P. de Medina, F. Delarue, J.J. Perie, A. Klæbe, J.C. Faye, Synthesis, binding and structure-affinity studies of new ligands for the microsomal anti-estrogen binding site (AEBS), *Bioorg. Med. Chem.* 8 (8) (2000) 2007–2016.
- [55] L. Yoder, The replacement of secondary hydroxyl groups by sulfonic acid substituents 1, *J. Org. Chem.* 20 (10) (1955) 1317–1321.
- [56] K.R. Beck, L. Telisman, C.J. van Koppen, G.R. Thompson 3rd, A. Odermatt, Molecular mechanisms of posaconazole- and itraconazole-induced pseudohyperaldosteronism and assessment of other systemically used azole antifungals, *J. Steroid Biochem. Mol. Biol.* 199 (2020), 105605.
- [57] P. de Medina, M.R. Paillasse, G. Segala, M. Voisin, L. Mhamdi, F. Dalenc, M. Lacroix-Triki, T. Filleron, F. Pont, T.A. Saati, C. Morisseau, B.D. Hammock, S. Silvente-Poirot, M. Poirot, Dendrogenin A arises from cholesterol and histamine metabolism and shows cell differentiation and anti-tumour properties, *Nat. Commun.* 4 (2013) 1840.
- [58] M. Record, M. Attia, K. Carayon, L. Pucheu, J. Bunay, R. Soules, S. Ayadi, B. Payre, L. Perrin-Cocon, F. Bourgaill, A. Lamaziere, V. Lotteau, M. Poirot, S. Silvente-Poirot, P. de Medina, Targeting the liver X receptor with dendrogenin A differentiates tumour cells to secrete immunogenic exosome-enriched vesicles, *J. Extra Vesicles* 11 (4) (2022), e12211.
- [59] L. Rajagopalan, J.N. Greeson, A. Xia, H. Liu, A. Sturm, R.M. Raphael, A. L. Davidson, J.S. Oghalai, F.A. Pereira, W.E. Brownell, Tuning of the outer hair cell motor by membrane cholesterol, *J. Biol. Chem.* 282 (50) (2007) 36659–36670.
- [60] P. de Medina, B.L. Payre, J. Bernad, I. Bosser, B. Pipy, S. Silvente-Poirot, G. Favre, J.C. Faye, M. Poirot, Tamoxifen is a potent inhibitor of cholesterol esterification and prevents the formation of foam cells, *J. Pharmacol. Exp. Ther.* 308 (3) (2004) 1165–1173.
- [61] L.C. King, R.M. Dodson, L.A. Subluskey, Preparation and structure of cholesteryl quaternary salts, *J. Am. Chem. Soc.* 70 (3) (1948) 1176.
- [62] B. Dayal, K. Rao, G. Salen, Microwave-induced organic reactions of bile acids: esterification, deformylation and deacetylation using mild reagents, *Steroids* 60 (6) (1995) 453–457.
- [63] F. Stellaard, K. von Bergmann, T. Sudhop, D. Lutjohann, The value of surrogate markers to monitor cholesterol absorption, synthesis and bioconversion to bile acids under lipid lowering therapies, *J. Steroid Biochem. Mol. Biol.* 169 (2017) 111–122.
- [64] B. Payre, P. de Medina, N. Boubekeur, L. Mhamdi, J. Bertrand-Michel, F. Terce, I. Fourquaux, D. Goudouneche, M. Record, M. Poirot, S. Silvente-Poirot, Microsomal antiestrogen-binding site ligands induce growth control and differentiation of human breast cancer cells through the modulation of cholesterol metabolism, *Mol. Cancer Ther.* 7 (12) (2008) 3707–3718.
- [65] P. de Medina, B. Payre, N. Boubekeur, J. Bertrand-Michel, F. Terce, S. Silvente-Poirot, M. Poirot, Ligands of the antiestrogen-binding site induce active cell death and autophagy in human breast cancer cells through the modulation of cholesterol metabolism, *Cell Death Differ.* 16 (10) (2009) 1372–1384.
- [66] P. de Medina, S. Silvente-Poirot, M. Poirot, Tamoxifen and AEBS ligands induced apoptosis and autophagy in breast cancer cells through the stimulation of sterol accumulation, *Autophagy* 5 (7) (2009) 1066–1067.
- [67] B. Sola, M. Poirot, P. de Medina, S. Bustany, V. Marsaud, S. Silvente-Poirot, J. M. Renoin, Antiestrogen-binding site ligands induce autophagy in myeloma cells

- that proceeds through alteration of cholesterol metabolism, *Oncotarget* 4 (6) (2013) 911–922.
- [68] G. Segala, M. David, P. de Medina, M.C. Poirot, N. Serhan, F. Vergez, A. Mougél, E. Saland, K. Carayon, J. Leignadier, N. Caron, M. Voisin, J. Chierier, L. Ligat, F. Lopez, E. Noguier, A. Rives, B. Payre, T.A. Saati, A. Lamaziere, G. Despres, J. M. Lobaccaro, S. Baron, C. Demur, F. de Toni, C. Larrue, H. Boutzen, F. Thomas, J. E. Sarry, M. Tosolini, D. Picard, M. Record, C. Recher, M. Poirot, S. Silvente-Poirot, Dendrogenin A drives LXR to trigger lethal autophagy in cancers, *Nat. Commun.* 8 (1) (2017) 1903.
- [69] J. Luo, L. Jiang, H. Yang, B.L. Song, Routes and mechanisms of post-endosomal cholesterol trafficking: a story that never ends, *Traffic* 18 (4) (2017) 209–217.
- [70] J. Ye, X. Xia, W. Dong, H. Hao, L. Meng, Y. Yang, R. Wang, Y. Lyu, Y. Liu, Cellular uptake mechanism and comparative evaluation of antineoplastic effects of paclitaxel-cholesterol lipid emulsion on triple-negative and non-triple-negative breast cancer cell lines, *Int. J. Nanomed.* 11 (2016) 4125–4140.
- [71] W. Liu, B. Liang, J. Zeng, J. Meng, L. Shi, S. Yang, J. Chang, C. Wang, X. Hu, X. Wang, N. Han, C. Lu, J. Li, C. Wang, H. Li, R. Zhang, D. Xing, First discovery of cholesterol-lowering activity of parthenolide as NPC1L1 inhibitor, *Molecules* 27 (19) (2022).
- [72] H. Liu, Y. Tian, K. Lee, P. Krishnan, M.K. Wang, S. Whelan, E. Mevers, V. Soloveva, B. Dedic, X. Liu, J.M. Cunningham, Identification of potent ebola virus entry inhibitors with suitable properties for in vivo studies, *J. Med. Chem.* 61 (14) (2018) 6293–6307.
- [73] M. Cote, J. Misasi, T. Ren, A. Bruchez, K. Lee, C.M. Filone, L. Hensley, Q. Li, D. Ory, K. Chandran, J. Cunningham, Small molecule inhibitors reveal Niemann-Pick C1 is essential for Ebola virus infection, *Nature* 477 (7364) (2011) 344–348.
- [74] J.E. Carette, M. Raaben, A.C. Wong, A.S. Herbert, G. Obernosterer, N. Mulherkar, A.I. Kuehne, P.J. Kranzusch, A.M. Griffin, G. Ruthel, P. Dal Cin, J.M. Dye, S. P. Whelan, K. Chandran, T.R. Brummelkamp, Ebola virus entry requires the cholesterol transporter Niemann-Pick C1, *Nature* 477 (7364) (2011) 340–343.
- [75] L. John, C. Verneris, H. Kwon, U. Elling, J.M. Penninger, A. Mirazimi, Redirecting imipramine against bluetongue virus infection: insights from a genome-wide haploid screening study, *Pathogens* 11 (5) (2022).
- [76] P. Ortega-Gonzalez, G. Taylor, R.K. Jangra, R. Tenorio, I. Fernandez de Castro, B. A. Mainou, R.C. Orchard, C.B. Wilen, P.H. Bringleb, J. Sojati, K. Chandran, M. Sachse, C. Risco, T.S. Dermody, Reovirus infection is regulated by NPC1 and endosomal cholesterol homeostasis, *PLOS Pathog.* 18 (3) (2022), e1010322.
- [77] M.A. Cuesta-Geijo, I. Garcia-Dorival, A. Del Puerto, J. Urquiza, I. Galindo, L. Barrado-Gil, F. Lasala, A. Cayuela, C.O.S. Sorzano, C. Gil, R. Delgado, C. Alonso, New insights into the role of endosomal proteins for African swine fever virus infection, *PLOS Pathog.* 18 (1) (2022), e1009784.
- [78] A. Krishnan, E.H. Miller, A.S. Herbert, M. Ng, E. Ndungo, S.P. Whelan, J.M. Dye, K. Chandran, Niemann-Pick C1 (NPC1)/NPC1-like1 chimeras define sequences critical for NPC1's function as a flavivirus entry receptor, *Viruses* 4 (11) (2012) 2471–2484.
- [79] E.M. Coleman, T.N. Walker, J.E. Hildreth, Loss of Niemann Pick type C proteins 1 and 2 greatly enhances HIV infectivity and is associated with accumulation of HIV Gag and cholesterol in late endosomes/lysosomes, *Virol. J.* 9 (2012) 31.
- [80] C. Vial, J.F. Calderon, A.D. Klein, NPC1 as a modulator of disease severity and viral entry of SARS-CoV-2, *Curr. Mol. Med.* 21 (1) (2021) 2–4.
- [81] R.A. Ballout, D. Sviridov, M.I. Bukrinsky, A.T. Remaley, The lysosome: a potential juncture between SARS-CoV-2 infectivity and Niemann-Pick disease type C, with therapeutic implications, *FASEB J.* 34 (6) (2020) 7253–7264.
- [82] K. Ohgane, F. Karaki, T. Noguchi-Yachide, K. Dodo, Y. Hashimoto, Structure-activity relationships of oxysterol-derived pharmacological chaperones for Niemann-Pick type C1 protein, *Bioorg. Med. Chem. Lett.* 24 (15) (2014) 3480–3485.
- [83] K. Ohgane, F. Karaki, K. Dodo, Y. Hashimoto, Discovery of oxysterol-derived pharmacological chaperones for NPC1: implication for the existence of second sterol-binding site, *Chem. Biol.* 20 (3) (2013) 391–402.
- [84] B. Kedjoud, P. de Medina, M. Oulad-Abdelghani, B. Payre, S. Silvente-Poirot, G. Favre, J.C. Faye, M. Poirot, Molecular characterization of the microsomal tamoxifen binding site, *J. Biol. Chem.* 279 (32) (2004) 34048–34061.
- [85] B.R. Roszell, J.Q. Tao, K.J. Yu, L. Gao, S. Huang, Y. Ning, S.I. Feinstein, C.H. Vite, S. R. Bates, Pulmonary abnormalities in animal models due to Niemann-Pick type C1 (NPC1) or C2 (NPC2) disease, *PLOS One* 8 (7) (2013), e67084.
- [86] V. Demais, A. Barthelemy, M. Perraut, N. Ungerer, C. Keime, S. Reibel, F. W. Pfrieger, Reversal of pathologic lipid accumulation in NPC1-deficient neurons by drug-promoted release of LAMP1-coated lamellar inclusions, *J. Neurosci.* 36 (30) (2016) 8012–8025.